AIAA 2004-2693

Computational Investigation of Wings with Miniature Trailing Edge Control Surfaces

Hak-Tae Lee and Ilan M. Kroo
Stanford University, Stanford, CA 94305

2nd AIAA Flow Control Conference
Jun 28–July 1, 2004/Portland, OR

Computational Investigation of Wings with Miniature Trailing Edge Control Surfaces

Hak-Tae Lee*and Ilan M. Kroo†
Stanford University, Stanford, CA 94305

Miniature trailing edge effectors (MiTEs) are small flaps (typically 1% to 5% chord) actuated with deflection angles near 90 degrees. The small size, combined with little required power and good control authority enables the device to be used for both high bandwidth control and conventional attitude control. Numerous experiments and computational simulations have been conducted for two dimensional airfoils with miniature flaps. However, the three-dimensional characteristics of these devices haven't been extensively investigated. The present study examines the three dimensional aerodynamics of MiTEs using an incompressible Navier-Stokes flow solver. The overall change in lift induced by the flap as well as the lift distribution along the span are investigated. In addition, the effect of gaps between the flaps is examined.

Introduction

DURING the past five years, as an innovative concept for aircraft control, miniature trailing edge control surfaces have been extensively researched, mainly at Stanford University, in conjunction with the Air Force Office of Scientific Research.[1–5] Miniature trailing edge effectors (MiTEs) are small flaps attached to the trailing edge of a wing and deflected near 90 degrees when actuated (Figure 1). The size of MiTEs usually ranges from 1 to 5 percent chord, about an order of magnitude smaller than conventional control surfaces.

MiTEs share their fundamental mechanism of aerodynamic force alteration with the Gurney flap. In the 1960s, it was discovered by the car racing community that a thin strip attached to the trailing edge of a race car spoiler to enhance bending stiffness also had an positive aerodynamic effect. The device was named after race car driver Dan Gurney who was among the first to make this observation. Since then, numerous wind-tunnel tests and numerical computations have been performed.[6–11] With a Gurney flap, the aerodynamic force alteration is produced by a small region of separated flow directly upstream of the flap, with two counter-rotating vortices downstream of the flap effectively modifying the trailing edge Kutta condition and resulting in finite pressure difference between the upper and lower surfaces at the trailing edge. This mechanism was first proposed by Liebeck[6] and later verified via flow visualizations[5,10,11] and CFD[3,7] simulations.

While the Gurney flap is a one piece fixed device, miniature trailing edge effectors are multi-piece actuated devices. Each flap is individually actuated in a digitized manner and can be commanded to one of the three possible positions: up, down, or neutral. Spanwise variation and interdigitated deflections can produce rolling, pitching, and yawing moments, as well as the control of specific structural modes.

Fig. 1 A perspective view of a conceptual wing with miniature flaps attached to the trailing edge

MiTEs have distinct advantages over conventional control surfaces. The most notable feature is the high bandwidth actuation enabled by their small size and inertia. Consequently, MiTEs can be used for high frequency aeroelastic control[2,4] as well as conventional attitude control with significantly reduced power requirement. In addition, because each flap has only three states, the feedback servo mechanism can be eliminated resulting in simpler structure and lower manufacturing cost. By installing large number of MiTEs along the trailing edge, enough redundancy can be provided for the fault-tolerant design.

The purpose of the present study is to investigate the three dimensional aspects of the aerodynamic behavior of MiTEs. In addition to the fundamental dimension of flap height, the spanwise length of an individual flap must also be determined. Also, small gaps between the flaps are required to accommodate the bending deflection of a wing. While the effects of height has been thoroughly investigated in numerous previous researches including Lee and Kroo,[3] there has not been significant published data on the spanwise

*Research Assistant, Aircraft Aerodynamics and Design Group, Department of Aeronautics and Astronautics, Stanford Universtiy. AIAA student member

†Professor, Department of Aeronautics and Astronautics, Stanford Universtiy, AIAA fellow.

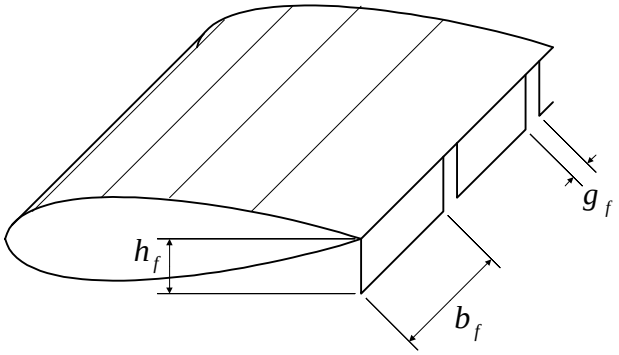

Fig. 2 Three major dimensions for MiTEs

length[5,12] or the gaps between flaps.[13]

In this paper, the impact of flap size and spacing on the lift distribution and the overall performance of the flap is investigated using a three dimensional incompressible Navier-Stokes solver.

Flow Solver

A three dimensional Reynolds-averaged Incompressible Navier-Stokes code, INS3D[14] is used. INS3D utilizes an artificial compressibility scheme that requires subiterations in the pseudo time domain to ensure a divergence free velocity field at the end of each physical time step. An upwind differencing scheme based upon flux-difference splitting is used for the convective terms, while a second-order central differencing is used for the viscous fluxes. The equations are solved using an implicit line relaxation scheme or generalized minimum residual method. The flow is assumed to be fully turbulent and the Spalart-Allmaras turbulence model with its good performance in separated regions away from the wall is used.

Geometry and Grid

Figure 2 shows a schematic diagram of MiTEs attached to the trailing edge of a wing. Three major dimensions regarding the MiTEs are indicated: the flap height h_f, length b_f, and gap g_f.

The flap aspect ratio is defined by the spanwise length b_f divided by the flap height h_f.

$$A_f = \frac{b_f}{h_f} \tag{1}$$

The wing is straight with no taper, and the boundary conditions for both ends are specified as symmetry planes such that the three dimensional effects relating the finite wing will not affect the result. For the computation of lift distribution and investigating the effect of aspect ratio, an NACA0012 airfoil is employed, while an HQ17 laminar flow airfoil is used to examine the effect of the gaps for comparison with the experimental result.

Computations were performed using a single zone, $197 \times 57 \times 73$ CH-grid as shown in Figure 3. Far field

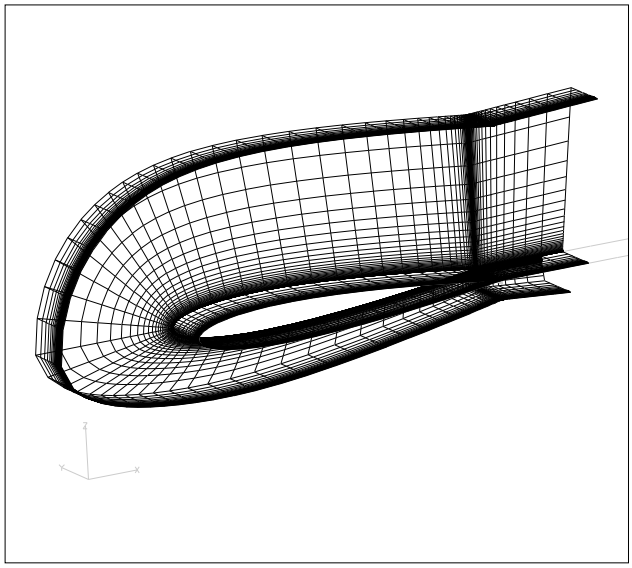

Fig. 3 Partial view of the CH-grid

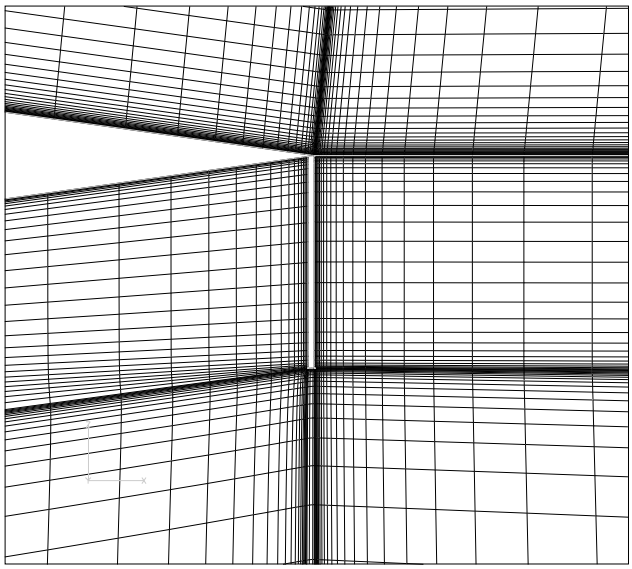

Fig. 4 A sectional view of the grid near the trailing edge

boundaries are located $15c$ from the airfoil for the inflow and $20c$ for the outflow, where c is the chord length. Minimum grid spacing in the direction normal to the solid wall is set to $2.0 \times 10^{-5}c$ to ensure an acceptable value of y^+ for the Spalart-Allmaras turbulence model.

The flaps are represented in the computational domain using the "iblank" function of INS3D. With "iblank", any point in the grid can be specified as a no slip surface or blanked out to be a hole region. Figure 4 shows the grid around the trailing edge and the flap.

Spanwise length of the flap

In this section, the effectiveness of the MiTEs with varying the flap length is investigated. The focus is on flaps with low aspect ratio less than four.

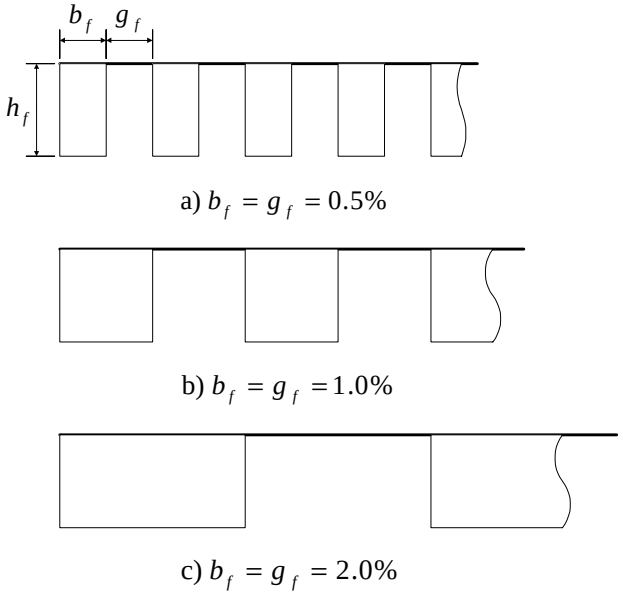

Fig. 5 Alternating flap and gaps where $h_f = 1\%c$ and $b_f = g_f$

Myose *et al*[12] performed wind tunnel tests with an NLF0414 straight wing at a Reynolds number of 1.2×10^6. In this experiment, h_f was $3.3\%c$ and three different spanwise lengths of 1/3, 2/3, and full span were tested. For the partial span flaps, the positions were changed from inboard to outboard. The increase in lift was generally proportional to the coverage of the flap, although flaps in the inboard position showed slightly better performance. Solovitz[5] performed a series of wind tunnel tests using MiTEs of $h_f = 1.5\%c$ with an aspect ratio of $A_f = 3.5$ at Reynolds number of 911,000. In this experiment, regardless of the configuration, the change in the lift was linear with respect to the total coverage.

Figure 5 shows the miniature flaps arranged in three different configuration with the flap height, h_f, fixed to $1\%c$. Each case consists of alternating flaps and gaps where the length of the flap and the gap size are identical. Hence, in all three cases, 50% of the wing is covered by flaps.

The grid dimensions in the spanwise direction are varied to examine the sensitivity of the results to the grid. Computations were performed at zero angle of attack and Reynolds number of one million. As the airfoil is symmetric, the computed value of C_L is also the lift increment ΔC_L.

Table 1 summarizes the results. Regardless of the b_f, and the number of spanwise grid points, the C_L is around half of the two dimensional value of 0.28. The results suggest that, if the gap size is comparable to the flap length, three dimensional effects are minor.

The next set of computations are performed for a wing with a fixed overall span between the symmetry planes and varying flap length as shown in Figure 6. The flap height is the same as the previous cases and

Table 1 Computed C_Ls for the configurations described in Figure 5

Number of grid points	a) $b_f = 0.5\%$ ($A_f = 0.5$)	b) $b_f = 1.0\%$ ($A_f = 1.0$)	c) $b_f = 2.0\%$ ($A_f = 2.0$)
8	0.1351	-	-
15	0.1379	0.1381	-
29	0.1394	0.1395	0.1338

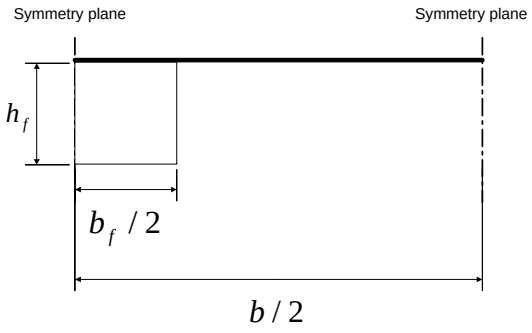

Fig. 6 For a fixed distance between the symmetry plane, the spanwise length of the flap, b_f is varied ($h_f = 1.0\%c$)

fixed to $1\%c$. Two different half spans, $4\%c$ and $16\%c$, are tested to examine whether the large clean area next to the flap has any effect on the flap performance. The C_L is plotted with respect to $b_f/2$ in Figure 7 for $b/2 = 4\%c$ and in Figure 8 for $b/2 = 16\%c$. In both cases, the C_L starts to deviate from its linear trend when $b_f/2$ becomes smaller than 1% which corresponds to the flap aspect ratio of 2. However, the deviation is mild and also a locally linear region is observed in Figure 7 when the $b_f/2$ is smaller than 0.5%. No apparent difference regarding the two different $b/2$'s can be found.

The two results in this section suggest that the effectiveness of the flap is remarkably linear with respect to its length b_f even at low aspect ratio. This linearity can provide designers with more freedom in selecting the spanwise length of flaps to fit their specific needs.

Lift distribution

In this section, the impact of a single flap on the spanwise lift distribution is investigated. As mentioned in the previous section, the overall change in the lift, ΔC_L, scales with the percentage of the wing span covered by the flap. However, the detailed lift distribution induced by a single flap has not been extensively examined. Resolving the lift distribution is important not only for understanding the underlying three dimensional aerodynamics of MiTEs, but also for practical applications. If the flap is used for attitude control such as an aileron, the lift distribution from each flap is required to compute the rolling moment. For aeroservoelastic application, it is also required to compute the structural deflection cause by the aero-

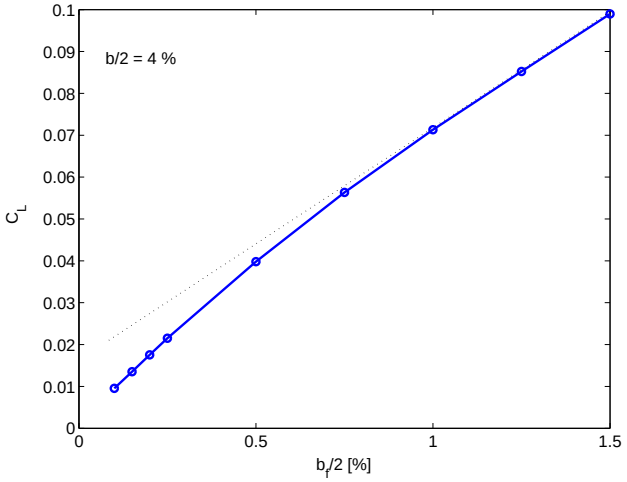

Fig. 7 C_L **with respect to** $b_f/2$ **for** $b/2 = 4\%c$ **(**$h_f = 1.0\%c$**)**

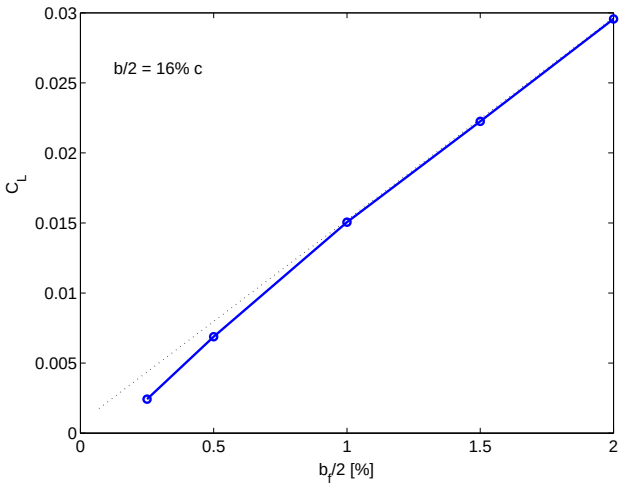

Fig. 8 C_L **with respect to** $b_f/2$ **for** $b/2 = 16\%c$ **(**$h_f = 1.0\%c$**)**

dynamic forces.

Lift distributions are computed for flap lengths ranging from 0.5% to 4.0%. Flap height, h_f, is fixed to $1\%c$ and the distance between the symmetry plane is selected to be $16\%c$. All computations are completed at zero angle of attack and a Reynolds number of one million.

Figure 9 shows the section C_l distribution computed by integrating the C_p at each spanwise stations. The peak value of section C_l at the middle of the flap ($y/c = 0$) is considerably lower than that of the two dimensional value. However, the lift is widely distributed along the span. Note that the symmetry boundary condition at both ends of the wing, which means the distribution plotted in Figure 9, is the superposition of all the lift distribution induced by the flaps placed $16\%c$ apart. The computation of lift distribution with much larger $b/2$ remains to be a future task.

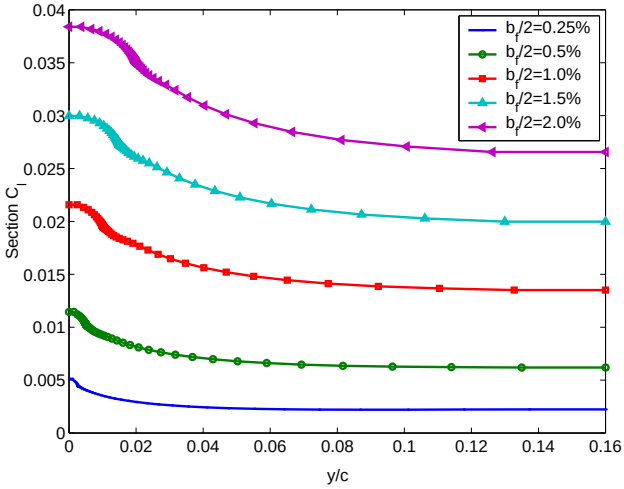

Fig. 9 Lift distribution. Section C_l **plotted with respect to** y/c **for** $h_f = 1\%$ **flap**

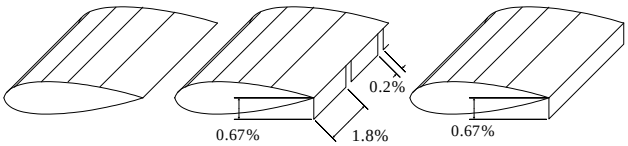

Fig. 10 The geometries for investigating the effect of gaps

Gaps between the flaps

The geometries used in the experiments by Bechert *et al*[13] are reproduced. An HQ17 laminar flow airfoil was chosen to reduce the drag of the baseline wing to emphasize the additional drag due to the flap. For the numerical simulations, a sharp trailing edge is assumed, while in the experiment, $0.33\%c$ thick blunt trailing edge was used. As observed by Lee and Kroo,[3] the effectiveness of the flap is a function of the flap height measured from the airfoil surface, so the flap height, h_f for the simulation is selected to be 0.67%. The flow is assumed to be fully turbulent in the simulation because currently INS3D cannot handle transitions and difficulties were encountered regarding convergence when the laminar flow option was selected. A Reynolds number of one million is used for both the experiment and the simulation. Figure 10 shows the three different configurations used for the analysis of gaps where a) indicates the baseline wing, b) indicates that there are gaps of $g_f = 0.2\%$ in between every flaps of $b_f = 1.8\%$, and c) showing the flap fully covering the trailing edge, which is equivalent to two dimensional configuration.

Figure 11 shows the $Cl - \alpha$ curve. At zero angle of attack, the wind tunnel test shows a ΔC_l of 0.25 from the baseline wing to the full span configuration. With gaps, the C_l decreased approximately 0.04. Computational results show a ΔC_l of 0.22 and a 0.02 decrease in the C_l with gaps. The computational result of around 10% reduction in lift is consistent with the previous

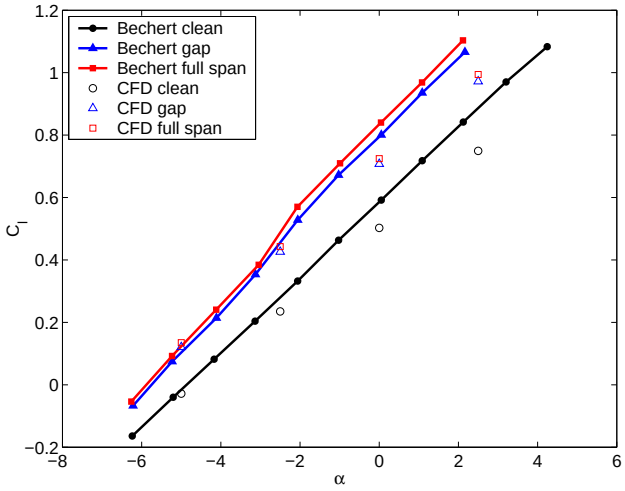

Fig. 11 $C_l - \alpha$ **curve**

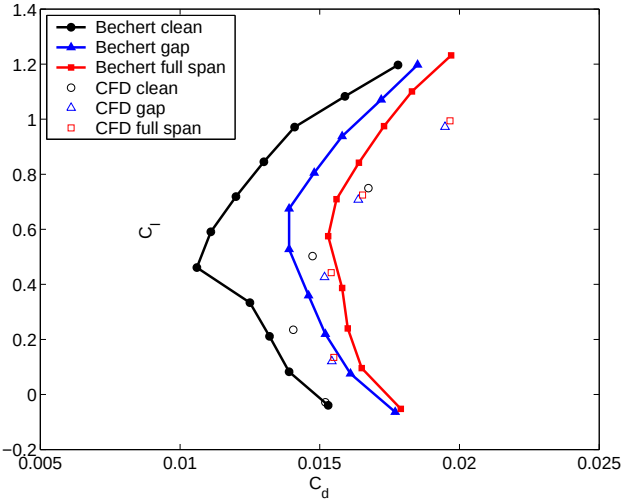

Fig. 12 Drag polar

section which states the ΔC_l is proportional to the portion of the trailing edge covered by the flap, since the gap covers 10% of the trailing edge. Both results show higher lift curve slope for the wing with flaps, but for each case, the computational results show lower lift curve slopes.

The drag polars are shown in Figure 12. Due to the turbulence flow assumed in the simulation, the laminar bucket is not observed in the computational results for the baseline wing. When the flap is attached, the computational results show slightly better agreement with the experimental data. However, in contrary to the experimental data which shows drag reduction of as much as 28%, the drag reduction obtained from the computation is less than 5%. As mentioned by Bechert, it is possible that the significant change in the drag related to the gap is due to an unsteady effect.

Conclusions

It has been shown that the aerodynamic force scale linearly with the spanwise length of the miniature flap up to $b_f/h_f \geq 2$. However, even for flap aspect ratio of lower than two, the flaps retain a considerable amount of effectiveness. The lift distribution is found to be widely spread along the span, even though the presence of the flap is highly localized. The notable reduction in drag by small gaps between the flaps is not observed from this computational study in which only steady state computations were performed. As mentioned by Bechert *et al*, this phenomenon could be an unsteady effect so that the drag without the gaps can be considerably higher than the one predicted by the steady CFD. Future work will involve time accurate simulations.

References

[1]Kroo, I. M., Eaton, J., and Prinz, F., "UAV Aeroelastic Control Using Redundant Microflaps," Afosr program review, 1999.

[2]Lee, H., Kroo, I. M., and Bieniawski, S., "Flutter Suppression for High Aspect Ratio Flexib Wings Using Microflaps," AIAA Paper 2002-1717, April 2002.

[3]Lee, H. and Kroo, I. M., "Computational Investigation of Airfoils with Miniature Trailing Edge Control Surfaces," AIAA Paper 2004-1051, Jan. 2004.

[4]Bieniawski, S. and Kroo, I. M., "Development and Testing of an Experimental Aeroelastic Model with Micro-Trailing Edge Effectors," AIAA Paper 2003-0220, Jan. 2003.

[5]Solovitz, S. A., "Experimental Aerodynamics of Mesoscale Trailing-Edge Actuators," Ph.d. thesis, stanford university, Dec. 2002.

[6]Liebeck, R. H., "Design of Subsonic Airfoils for High Lift," *Journal of Aircraft*, Vol. 15, No. 9, Sept. 1978.

[7]Jang, C. S., Ross, J. C., and Cummings, R. M., "Computational Evaluation of an Airfoil with a Gurney Flap," AIAA Paper 92–2708, June 1992.

[8]Storms, B. L. and Jang, C. S., "Lift Enhancement of an Airfoil Using a Gurney Flap and Vortex Generators," *Journal of Aircraft*, Vol. 31, No. 3, June 1994.

[9]Giguere, P., Lemay, J., and Dumas, G., "Gurney Flap Effects and Scaling for Low-Speed Airfoils," AIAA Paper 95–1881, June 1995.

[10]Jeffrey, D., Zhang, X., and Hurst, D. W., "Aerodynamics of Gurney Flaps on a Single-Element High-Lift Wing," *Journal of Aircraft*, Vol. 37, No. 2, 2000, pp. 295–301.

[11]Zerihan, J. and Zhang, X., "Aerodynamics of Gurney Flaps on a Wing in Ground Effect," *AIAA Journal*, Vol. 39, No. 5, May 2001, pp. 772–780.

[12]Myose, R., Papadakis, M., and Heron, I., "Gurney Flap Experiments on Airfoils, Wings, and Reflection Plane Model," *Journal of Aircraft*, Vol. 35, No. 2, Mar.-Apr. 1998.

[13]Bechert, D. W., Meyer, R., and Hage, W., "Drag reduction of airfoils with miniflaps - Can we learn from dragonflies?" AIAA Paper 2000-2315, June 2000.

[14]Rogers, S. E. and Kwak, D., "An Upwind Differencing Scheme for the Time Accurate Incompressible Navier-Stokes Equations," AIAA Paper 88–2583, June 1988.